Heliyon 9 (2023) e17597

Contents lists available at ScienceDirect

Heliyon

journal homepage: www.cell.com/heliyon

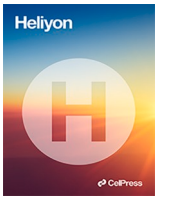

Microbially induced calcium carbonate precipitation in fossil consolidation treatments: Preliminary results inducing exogenous *Myxococcus xanthus* bacteria in a miocene *Cheirogaster richardi* specimen

Silvia Marín-Ortega [a,c,*], M. Àngels Calvo i Torras [b], Manuel Ángel Iglesias-Campos [c]

[a] *Conservation-Restoration Department, Escola Superior de Conservació i Restauració de Béns Culturals de Catalunya, Carrer d'Aiguablava, 109-113, 08033, Barcelona, Spain*

[b] *Applied and Environmental Microbiology Research Group. Department of Animal Health and Anatomy, Faculty of Veterinary Medicine, Universitat Autònoma de Barcelona, Travessera dels Turons, Edifici V. 08193, Bellaterra, Spain*

[c] *Heritage Conservation-Restoration Research Group. Arts and Conservation-Restoration Department, Faculty of Fine Arts, Universitat de Barcelona, Carrer de Pau Gargallo, 4, 08028, Barcelona, Spain*

A R T I C L E I N F O

Keywords:
Microbially induced calcium carbonate precipitation
Conservation
Fossil
Myxococcus xanthus
paleontological heritage
Bioconsolidation

A B S T R A C T

This research paper proposes Microbially Induced Calcium Carbonate Precipitation (MICP) as an innovative approach for palaeontological heritage conservation, specifically on deteriorated carbonate fossils. Due to its efficiency in bioconsolidation of carbonate ornamental rocks, *Myxococcus xanthus* inoculation on carbonate fossils was studied in this research.

Treatment was tested on nine fossil samples from decontextualized fragments of *Cheirogaster richardi* specimens (Can Mata site, Hostalets de Pierola, Catalonia, Spain). The main objective was to evaluate whether treatment with *Myxococcus xanthus* improved fossil surface cohesion and hardness and mechanical strength without significant physicochemical and aesthetic changes to the surface. Chemical compatibility of the treatment, penetration capacity and absence of noticeable changes in substrate porosity were considered as important issues to be evaluated.

Samples were analysed, before and after treatment, by scanning electron microscopy, weight control, spectrophotometry, X-ray diffraction analysis, water absorption analysis, pH and conductivity control, Vickers microindentation and tape test. Results show that hardness increases by a factor of almost two. Cohesion also increases and surface disaggregated particles are bonded together by a calcium carbonate micrometric layer with no noticeable changes in surface roughness. Colour and gloss variations are negligible, and pH, conductivity and weight hardly change. Slight changes in porosity were observed but without total pore clogging.

To sum up, results indicate that *Myxococcus xanthus* biomineralisation is an effective consolidation treatment for carbonate fossils and highly compatible with carbonate substrates. Furthermore, bacterial precipitation of calcium carbonate is a safe and eco-friendly consolidation treatment.

* Corresponding author. Conservation-Restoration Department, Escola Superior de Conservació i Restauració de Béns Culturals de Catalunya, Carrer d'Aiguablava, 109-113, 08033, Barcelona, Spain.

E-mail addresses: marinortegasilvia@gmail.com (S. Marín-Ortega), mariangels.calvo@uab.cat (M. Àngels Calvo i Torras), manuel.iglesias@ub.edu (M.Á. Iglesias-Campos).

https://doi.org/10.1016/j.heliyon.2023.e17597
Received 24 June 2022; Received in revised form 20 June 2023; Accepted 21 June 2023
Available online 22 June 2023

1. Introduction

Traditionally, consolidation of palaeontological remains has been accomplished through the use of strengthening substances like resins, adhesives and waxes. This technique, which has been documented since the 19th century [1–3], was developed concurrently with the consolidation of monumental stone structures [4–6] and archaeological assets [7,8].

At present, paleontological consolidation primarily involves polymer impregnation, particularly acrylic resins [9–14]. This process, otherwise commonly known as palaeontological preparation, is designed to maintain fossil morphology and enhance hardness for easier fossil manipulation for histopathological, histomorphometric, taphonomic and taxonomic research works [10,15].

Even though polymers provide an efficient hardening solution for the immediate requirements, they provoke brightness and colour changes and can affect future analysis [10,16,17]. Polymers can also chemically alter the substrate, increase its weight and generate film surface formation with different shrinkage-dilation coefficients, leading to delamination, disruption, pore clogging [18], and alterations in water and gas behaviour [19–22]. For these reasons, alternative and compatible treatments should be explored.

Fossil bones consist primarily of a mineral fraction ranged 60–70 wt%, principally carbonate–hydroxyapatite ($Ca_5(PO_4)_{3-x}(CO_3)_xOH_{x+1}$) [23]. Therefore, inorganic consolidations would be preferred to resins because of their physicochemical affinity with mineral substrates [24].

While they are buried, empty spaces form in bone remains when organic material, such as cells, blood vessels and collagen (20–30 wt%) decays [25]. Hydroxyapatite may also leach out leaving new spaces and demineralising the remains [21].

These new spaces are filled up over millions of years through the deposition of minerals from surrounding sediments and groundwater [25,26] and by bacterial mineral new formation, facilitated by a favourable combination of sedimentological, geochemical and microbial conditions [27–32]. This process, known as fossil-diagenesis or fossilisation by pseudomorphosis and permineralization, depends on hydrology and the burial environment [26,33]. It also depends on bone-environment relationship: mineral leaching, collagen loss, ion exchange, microbial action and seepage by soil compounds [21].

Most fossils are mainly permineralized by calcium carbonate [34]. Simultaneously, while buried, bones continue to be demineralised affecting their mechanical properties. Consequently, a compatible way to consolidate fossil bones might involve the in-situ growth of $CaCO_3$ crystals [35].

A method to induce calcium carbonate in carbonate substrates would occur via bacterial carbonatogenesis. In the 1970s, Boquet, Boronat and Ramos-Cormenzana proved that the majority of heterotrophic soil bacteria were able to precipitate calcium carbonate [36].

However, it was in the 1990s when Adolphe, Castanier, Loubière and Le Métayer-Levrel proposed the use of Microbial Induced Calcium Carbonate Precipitation (MICP) for the purpose of consolidating ornamental stone [37]. Since that time, researchers have conducted tests on this form of bioconsolidation on ornamental stone [24,38–42], plasters [20,43] and wall paintings [44].

Bioconsolidation replicates a process undertaken by nature for countless millennia with many carbonate rocks originating in MICP [45–47]. Furthermore, it also reproduces some autogenous microbial permineralization caused during the fossilisation process [28]. It is worth noting that the most prevalent autogenous fossilisation minerals are calcium carbonate and calcium phosphate, both common in fossil bones and burial environment [26,48]. Indeed, the majority of fossils consist of biomineralized remains [28] and, even though the initial taphonomic modifications are initiated by fossil-specific bacteria and bone mineralogy, the most notable diagenetic changes are primarily driven by the influence of soil microorganisms [33].

For all these reasons, MICP is proposed in this research as a viable and appropriate method for carbonate paleontological heritage consolidation. Even though this consolidation treatment has been tested with different bacterial strains and culture media, the main procedures consist of bacterial inoculation accompanied by a calcium and carbonate rich media [24,39–41,49], or in direct stimulation of the substrate's microbiota itself by using a carbon and calcium source rich medium [20,42,50–52].

Rodríguez-Navarro et al. [24] found that *Myxococcus xanthus*, under appropriate conditions, had a high capacity for precipitating calcium carbonate due to its metabolic activity. In addition, they found that *M. xanthus* outperformed bacteria tested in other research studies in several ways [38–41]. Treatment promoted a good mechanical strength without plugging the pores, i.e. allowing gas exchange, and the stone colour was not modified. Treatment also showed a better penetration and adhesion between newformed crystals and substrate. In addition, when samples were dried, there was no bacteria fructification and, therefore, no uncontrolled bacterial growth could appear when treatment was completed [24,49,53]. Several studies have proven the effectiveness of *M. xanthus* in ornamental and architectural stone consolidation from 1996 [24,49,54–57].

For the above reasons, present research has tested *M. xanthus* calcium carbonate precipitation on fossil carbonated remains, specifically on miocene *Cheirogaster richardi* specimen fragments. The main aim of this study is to ascertain the *M. xanthus* capacity to establish a cohesive carbonate matrix in fossil porous systems, considering treatment viability, applicability and effectiveness. Cohesion and hardness improvements must be also determined without causing significant physicochemical and aesthetic changes on fossil remains. In addition, the evaluation of the issues of chemical compatibility, penetration capacity and the absence of noticeable changes in substrate porosity were considered relevant issues to be evaluated.

Results would allow an alternative treatment for carbonate fossil consolidation that has not been conducted before. Additionally, MICP is a recognized safe and eco-friendly methodology [58].

2. THEORY: *Myxococcus xanthus* metabolic activity involved in MICP

M. xanthus cell walls possess carboxyl and hydroxyl groups that undergo deprotonation in an alkaline environment, resulting in the

generation of negative charges. Negative charges exhibit a pronounced electrostatic attraction to metal cations in aqueous environments [59]. Since metabolic processes do not necessitate large quantities of calcium ions, any surplus accumulates outside the cell [60]. Owing to the influence of electrostatic attraction forces, calcium ions remain adhered to the bacterial cell membrane. Once attached to the cell walls, calcium ions form bonds with carbon found in the medium, consequently leading to the generation of calcium carbonate surrounding the cell [24,54,61]. This mechanism is an evolutionary adaptation in which bacteria can regulate cellular ionic balance and provide structural support structures both inside and outside the cell [19].

In regular equilibrium reaction, once a specific level of saturation in solution is reached [24,62] calcium carbonate precipitation occurs as follows: $Ca^{2+} + CO_3^{2-} \leftrightarrow CaCO_3$. In addition, CO_3^{-2} production in alkaline conditions increases as it is pH-dependent [63,64] by the following equilibrium reaction [65]:

$$HCO_3^- \leftrightarrow CO_3^{2-} + H^+$$

$$HCO_3^- + OH^- \leftrightarrow CO_3^{2-} + H_2O$$

It is well known that heterotrophic metabolic bacterial processes raise the pH via the release of ammonia and various other metabolites [33,47]. In fact, *M. xanthus* metabolic activity implies NH_3 production by amino acid oxidative deamination. That is why culture media involved in the process should contain an amino-acid-rich pancreatic digest, as a carbon and nitrogen source [24]. A non-use of carbohydrates and glucoses as carbon supplies, will significantly reduce the likelihood of acid production [50]. Inhibiting the acid production, medium alkalinity is maintained, which means carbonate precipitation increases.

Amino acid carbon source also prevents fungus or acid-producing bacteria proliferation [50] that can affect the fossil by acid dissolution. Furthermore, the applied medium should have a slightly alkaline pH (a pH 8 buffer), so it can act against pH decreases. In conclusion, *M. xanthus* inoculated calcifying media should have a high calcium ions saturation and alkaline conditions favouring carbonaceous precipitation [24].

In addition to the direct biomineralisation mechanism explained above, bacteria also biomineralizes indirectly [64]. It has been demonstrated that organic dead bacteria networks and extracellular polymeric substances (EPS) act as a calcification matrix [66]. In fact, these surfaces help to bind ions from ionic solutions acting as nucleation areas for mineral deposition [61,67–70]. Both processes feed back into each other. As the number of cells increases, so does the number of crystallization nuclei, resulting in a faster precipitation of calcium carbonate [50]. Moreover, these new carbonates contain a certain percentage of organic bacterial matter, which means that the organic part can harden calcite, as occurs in sea shells [71].

3. Materials and methods

3.1. Bacterial strain and culture media

Microorganism employed in the study was *M. xanthus* from Spanish Type Culture Collection (CECT), strain number 422. *M. xanthus* is a gram-negative, heterotrophic and aerobic soil myxobacterium. Obviously, bacteria inoculated must be non-pathogenic to be safe to both conservators and heritage [72]. *M. xanthus* was precultured in CT media: 1% [wt/vol] Bacto Casitone, 0.1% [wt/vol] $MgSO_4{\cdot}7H_2O$ in a 10 mM phosphate buffer at pH 6.5 as described in Rodríguez-Navarro et al. [24]. Preculture media underwent sterilisation via autoclaving at 120 °C. *M. xanthus* was incubated at a temperature of 28 °C for a duration of 48 h to achieve an approximate density of 3×10^9 cells/mL.

For bioconsolidation experiments, 2% [wt/vol] of the previous *M. xanthus* culture was inoculated in sterile liquid media M − 3P [1% Bacto Casitone, 1% $Ca(CH_3COO)_2{\cdot}4H_2O$, 0.2% $K_2CO_3{\cdot}1/2H_2O$ in a 10 mM phosphate buffer, pH 8], as described in Rodríguez-Navarro et al. [24]. Part of M − 3P medium was gelled without inoculum by 2% [wt/vol] purified agar.

3.2. Fossil samples

The procedure involved the preparation of nineteen fossil sample cubes from a late miocene *Cheirogaster richardi* giant tortoise plastron. Nine samples were used for bioconsolidation tests, three for simultaneous pH analysis and seven for control measurements. Plastron was selected because it had the same thickness and characteristics in the whole area. All samples were extracted from the surface area. The fossil bone employed was found in Hostalets de Pierola (Can Mata site, Catalonia, Spain) in 2009, along with 5000 other fossils during a recycling plant construction works, and was chosen because the fragment was very carbonated (SEM and Lindholm Test verification) and because it showed typical surface deterioration. Among all the fossils, 200 *Cheirogaster richardi* remains were found but only 37 specimens were complete and in good condition [73].

Selected bone fragment was still embedded in a large and compacted clay block matrix. To facilitate fragment extraction, controlled capillary hydration was needed. Fossil blocks were cut with a diamond saw into $2 \times 2 \times 1$ cm approximately. The selected size and number of samples are justified by the total available piece of fossil. It was not feasible to sacrifice a large fragment given its heritage importance.

Samples were sterilized in two steps: 10 min of immersion in 70:30 ethanol-water solution followed by three 30-min ultraviolet (UVC) sterilisation cycles. Tyndallization or autoclaving sterilisation was not possible in this case because samples cannot withstand the process.

3.3. Bioconsolidation tests

Nine fossil samples were inoculated with 2% [wt/vol] *M. xanthus* culture in sterile liquid M-3P media. In order to mimic a realistic fossil consolidation treatment, samples were not treated by immersion but surface-treated. Subsequently, inoculated M-3P media was applied by dropping until all surface saturation was achieved, homogenised each time with a Vortex®. Immediately, gelled M-3P media was applied on the top of inoculated samples to ensure nutrient and water source during the 7-day treatment (Fig. 1a). This innovation can favour better carbonation by keeping bacteria alive longer.

Samples were incubated at 28 °C for 7 days. A daily inoculated M-3P was applied to ensure bacterial activity during the required 7 days. At the end of incubation, samples underwent three rinses with distilled sterile water and were dried at 37 °C for three days. After drying, samples were left to cure for 90 days.

Three control tests were also performed with uninoculated M-3P media. *M. xanthus* corroboration and contamination tests were carried out by swab surface sampling when treatment was finished. Swap samples were inoculated on Tryptic Soy Agar and Mac-Conkey agar plates and incubated for 24–48 h at 28 °C and 37 °C (Fig. 1b and c). Swap samples were also inoculated on Saboraud dextrose Agar with chloramphenicol and incubated at 28 °C for five-seven days. Gram staining was performed, and a biochemical miniaturised Analytical Profile Index (API) test was carried out to identify genus and species.

3.4. ATP analysis

ATP quantification, serving as a bioindicator of microbial activity, was conducted using a Hygiena SystemSURE Plus® luminometer [74–76].

ATP assay was used to check bacteria viability before, during and after treatment. Before treatment, ATP assay can corroborate a good viability in inoculated M-3P solution and allows the checking of fossil sample sterilisation before inoculation. During treatment, viability could be checked in less than a minute to determine whether treatment is properly developed or if a booster with more inoculum is needed. After treatment, ATP assay helps to monitor live bacteria remains on the fossil surface. In this regard, bacterial proliferation could provoke undesirable microbiota growth, damaging heritage substrate [53,77]. To minimize this risk, it is advisable to conduct comprehensive rinsing and drying procedures after treatment, followed by monitoring for potential bacterial proliferation.

During this experiment, AquaSnap® and UltraSnap® ATP devices were utilized. To differentiate free ATP from non-viable fragmented cells, it is necessary to employ two distinct devices [75,76,78]; in this particular case AquaSnap Total® and AquaSnap Free®. It is crucial to discriminate extracellular or free ATP in this context, so both devices had to be used in each sample. 100 µl of inoculated M-3P media was collected with AquaSnap® just after Vortex® agitation before each application on fossils. UltraSnap® ATP swab devices were used for viability surface monitoring during and after treatment.

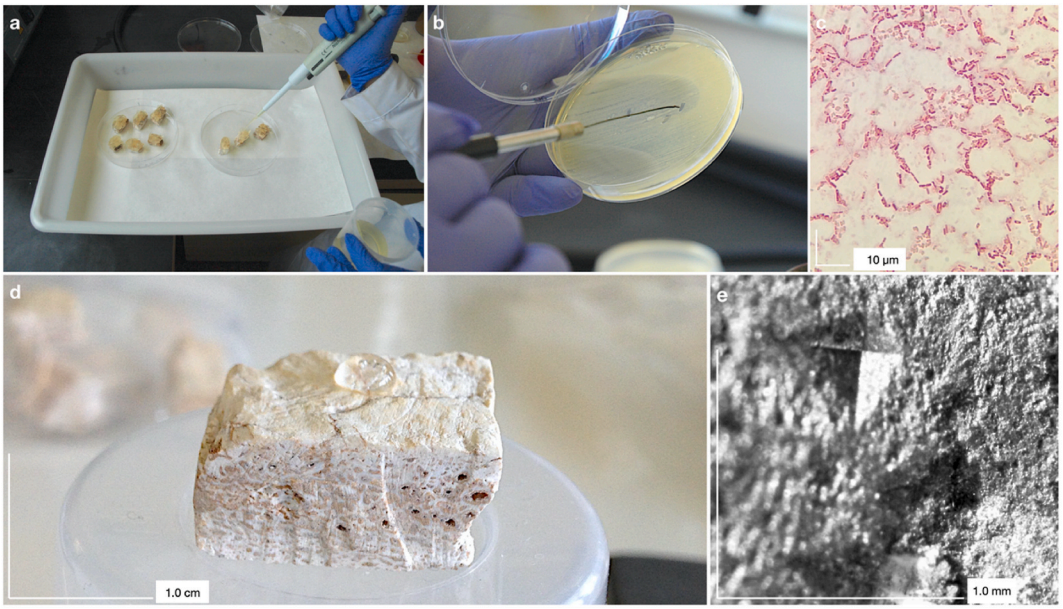

Fig. 1. Experimental process images. (a) *M. xanthus* bioconsolidation tests. (b) Corroboration and contamination tests cultured and incubated for 48 h at 28 °C. (c) *M. xanthus* corroboration result microscope 1000x image after gram staining. (d) 50 µl water drop absorption analysis before treatment. (e) Microindenter imprint on fossil sample to determine Vickers microindentation hardness analysis.

3.5. Conductivity and pH analysis

Conductivity and pH on the surfaces of the samples were determined using 5% low electroendosmosis (EEO) pure agarose in distilled water discs of Ø 3 mm and Ø 8 mm respectively. Discs were placed on the samples surfaces for 20 min and then read by using Horiba Laquatwin® solid conductivity meter and PCE®-228S ERH-115 surface pH meter.

Three measurements per sample were taken before and after treatment to analyse possible pH and conductivity changes. Arithmetic averages and standard deviation were calculated. Pre-treatment data were important to achieve a fossil-safe bioconsolidation because they determined the use of slightly alkaline pH and isotonic conductivity as close as possible to the original fossil to prevent calcium carbonate and calcium phosphate solubility damage.

Bacterial metabolic activity results in carbon dioxide and ammonia production. Ammonia increases pH and calcium carbonate precipitation occurs in the case of oversaturation [79]. Therefore, pH increases can be indicative of biocarbonation. Simultaneous tests in test tubes were carried out to evaluate possible pH changes during treatment because this was very difficult to achieve on the surface of the fossil. In this case, three control samples were immersed in 50 mL of inoculated M-3P in order to evaluate daily pH changes on liquid media.

3.6. Weight increase analysis

Bacterially treated samples were weighed before and after treatment using a Sartorius® Basic precision balance with a sensitivity of 0.0001 g to observe weight increase in each case. Three measurements per sample were performed. Arithmetic averages and standard deviation were calculated. The calculation of weight increase involved subtracting the average initial weight from the average final weight in each sample at the end of incubation.

3.7. Spectrophotometry analysis

All samples were analysed before and after bioconsolidation to evaluate possible treatment colour changes. Analyses were carried out with a Konica Minolta® CM 2600d spectrophotometer and SCI-CIELAB L*a*b* coordinates. Measurements were taken with Ø 8 mm mask, specular component included, D65 illuminance and 10° observer angle. Three measurements per sample were taken in three defined and fixed areas. These three measurements mean the complete reading of the samples' surface. Arithmetic average, standard deviation and Delta coordinates were calculated (ΔL^*, Δa^*, Δb^* and $\Delta E^* = [\Delta L^{*2} + \Delta a^{*2} + \Delta b^{*2}]1/2$).

Colour change tolerance index was set at $\Delta E^* = 5$, the point at which it starts to become visible to the human eye [80–82].

3.8. SEM analysis

Four control untreated samples were analysed by scanning electron microscopy (SEM FEI QUANTA 200 EDAX) to examine the original fossil morphology on the internal perpendicular sections (n = 2) and on the surface (n = 2).

Induced calcium carbonate penetration depth and compositional and textural changes were also observed in all treated samples. All samples were resin mounted and observed with Backscattered Electron Image (BEI) and Secondary Electron Image (SEI).

To determine the thickness of the layer formed during bioconsolidation, nine measurements per sample were performed and arithmetic means and standard deviations were calculated.

Using the EDX X-ray detector, spot microanalyses were carried out for major elements identification.

3.9. Powder X-ray diffraction analysis

To determine the fossil and the newly-formed layer's composition, Powder X-ray Diffraction (PXRD) analysis was performed to identify crystalline phases. Three untreated samples and three treated samples were analysed. For fossil samples analysis, the original untreated cortical surface was pulverised. For bioconsolidated samples analysis, the most superficial layer possible was scraped off and ground. Analysis was performed using a PANalytical X'Pert diffractometer equipped with a PIXcel^{1D} detector. Cu Kα radiation (λ = 1.5419 Å) was used and the powder patterns were measured in the range 5-60° 2θ. Crystalline phase identification was carried out by comparison with the Powder Diffraction File (PDF) patterns using the HighScorePlus program. The relative mass fractions of calcite and hydroxyapatite were calculated using the RIR method with the RIR values from PDF patterns (01-072-1652 for calcite and 01-086-0740 for hydroxyapatite).

For fossil samples analysis, the original untreated cortical surface was pulverised. For bioconsolidated samples analysis, the most superficial layer possible was scraped off and ground.

3.10. Drop absorption analysis

Hydric properties changes were performed by drop absorption analysis. The absorption time of 50 μl water drop was recorded and evaluated before and after biomineralisation (Fig. 1d). Pore clogging and accessible porosity changes can be assessed indirectly with this analysis.

Nine repetitions were performed on each sample. Samples were dried at 50 °C for 48 h prior to each repetition to achieve the same absorption conditions each time. A 50 μl water was dropped on all samples at 1 cm distance and complete absorption time was

measured with a chronometer. Arithmetic averages and standard deviation were calculated.

3.11. Vickers microindentation hardness analysis

Control and bioconsolidated sample surfaces were analysed using a Galileo® ISOSCAN OD microindenter. Microindentation was performed on the nine bioconsolidated samples and on four control untreated samples to determine the original values prior to consolidation. Microindentation cannot be performed before and after treatment on the same samples because they would be destroyed before bioconsolidation experiments. Samples were coated with graphite and 1-g force (9.807 mN) was applied on five different and fixed areas per sample (Fig. 1e). Arithmetic averages were calculated to determine the Vickers hardness (HV) average for each sample and also standard deviations.

Since fossil samples had an irregular surface, the microindenter could not directly calculate the values. The imprint left by the microindenter was measured using a 200 × DinoLite® digital microscope in order to calculate Vickers mathematical formula. Hardness results were expressed in kg/mm^2.

3.12. Disaggregation tape test

Fossil surface disaggregation was analysed before and after treatment by removable adhesive tape test. One tape test was performed per sample because a significant number of particles can be extracted in a single application. Adhesive strips of the same size and weight were applied to sample surfaces. Each strip was removed after 5 s and weighed on a Sartorius® Basic precision balance with a sensitivity of 0.0001 g. As the weight of the adhesive strips is already known, the weight difference corresponds to the detached fossil surface particles. Subtraction between the detached particles' weight before and after treatment shows whether the treatment improves surface cohesion.

4. Results

4.1. Bacterial monitoring

Before treatment, ATP assay verified good viability in bacterial pre-culture. In this study, results obtained were between 4000 and 7000 RLU. These values correspond, according to total viable bacteria count plates, to a range of 2×10^9 cells/mL to $4{,}3 \times 10^9$ cells/mL. ATP assay also confirmed fossil samples sterilisation before inoculation. Results obtained were 0 RLU.

During treatment, inoculated M-3P solution viability was ATP checked to determine if treatment needed to be reinforced with more

Sample	Initial Cond 1 (µS)	Initial Cond 2 (µS)	Initial Cond 3 (µS)	Standard Deviation (µS)	Mean Initial Conductivity (µS)	Final Cond 1 (µS)	Final Cond 2 (µS)	Final Cond 3 (µS)	Standard Deviation (µS)	Mean Final Conductivity (µS)	Increase (µS)	Total Increase Standard Deviation (µS)	Multiplies by	% of increase	Total % of Increase Standard Deviation
B-D2	176	175	177	1	176	329	331	330	1	330	154		1,88	87,50	
B-D4	242	241	238	2	240	461	460	460	1	460	220		1,92	91,54	
B-D6	163	161	164	2	163	390	390	389	1	390	227		2,4	139,55	
B-O1	189	188	189	1	189	380	380	380	0	380	191		2,01	101,41	
B-O2	168	170	169	1	169	329	329	327	1	328	159		1,94	94,28	
B-O3	196	196	198	1	197	430	428	431	2	430	233		2,18	118,47	
B-SEM1	177	179	178	1	178	348	347	347	1	347	169		1,95	95,13	
B-SEM2	200	201	201	1	201	448	448	448	0	448	247		2,23	123,26	
B-SEM3	220	220	220	0	220	425	424	424	1	424	204	34,02	1,93	92,88	17,92
AVERAGES				1					1		201		2,05	104,89	

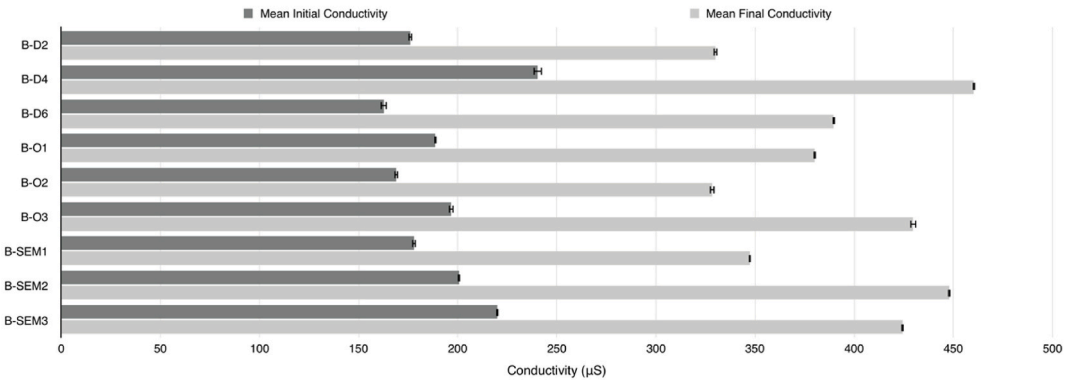

Fig. 2. Above: initial and final conductivity data of all samples and their statistics. Below: conductivity variations after *M. xanthus* treatment: initial and final mean conductivity for each sample.

inoculum. On the first 4 days, RLU values increased about 1800 RLU. From the fifth day viability started to decline and a booster was performed.

At the end of treatment, swab surface sampling showed bacteria suitability developed during treatment. *M. xanthus* corroboration and contamination tests were carried out with Analytical Profile Index (API) biochemical miniaturised test. Results confirmed a massive presence of *M. xanthus* in all the samples. Regarding contaminations, no other bacteria grew on samples.

After treatment, ATP assay confirmed no live bacteria remains on fossil surfaces. Following the rinsing and drying process, ATP monitoring reported 0 RLU data. The same results recurred for the following 10 days and 12 weeks.

4.2. Conductivity and pH analysis

All pH measurements remained stable at pH 8 in all samples before and after treatment, without variations. Regarding conductivity (Fig. 2), during the three repetitions performed on the nine samples variability has been very low, with a standard deviation from 0 to 2 μS, with a standard deviation mean of 1 μS. Conductivity increased in all cases after consolidation experiments. Results showed that conductivity increases between 154 and 247 μS with an average of 201 μS and with a standard deviation of 34,02 μS. Results reported an increase between 87.50% and 139.55%, with a total arithmetic average of 104.89% and a standard deviation of 17,92%.

Simultaneous test tube analyses revealed pH increases during treatment. Results showed a progressive gain from pH 8 to pH 8.4 on the fifth day of treatment. On the sixth day pH decreases to pH 8.2, and on the seventh day to pH 8.1 (Fig. 3).

4.3. Weight increase analysis

Weight increases were observed in all samples (Fig. 4). During the three repetitions performed on the nine samples, variability was very low, with a standard deviation from 0.0001 to 0.0010 g and a standard deviation mean of 0.0005 g. The weight increase ranged between 0.0196 and 0.0539 g with an average of 0.0321 g and a standard deviation of 0.0102 g. In percentage terms, the increase ranged between 0.27% and 0.96%, with a total arithmetic average of 0.44% and a standard deviation of 0.20%.

4.4. Spectrophotometry analysis

During the three measurements performed on the nine samples, variability was very low, with a standard deviation from 0 to 0.25 points and a standard deviation mean of 0.04 points. Initially samples were very close to white, with L* values between 77 and 88, a* values between 1 and 4, and b* values between 8 and 16 (a clear white with some red and brown tones due to slight clay traces). After treatment (Fig. 5), when Delta coordinates were calculated (ΔL*, Δa*, Δb* and ΔE*), luminance changes (ΔL*) were irrelevant. Five samples darkened slightly and four became lighter, but values below $\Delta E^* = 5$ indicate that changes cannot be seen by the human eye [80–82]. ΔE* data range between 1.7 and 5.91 with a total arithmetic average of 3.7 and a standard deviation of 1.45 points.

Almost all samples increased their value in a* and b* parameters, tending to veer towards yellow and red, but within the imperceptible range (Fig. 5). Two samples showed perceptible changes to the human eye, since $\Delta E^* > 5$, but only by a few tenths ($\Delta E^* = 5{,}12$; $\Delta E^* = 5{,}91$).

Fig. 5 shows ΔL*, Δa*, Δb* and ΔE* coordinates. Samples close to 0 have hardly changed at all. The $\Delta E^* > 5$ data are located in the

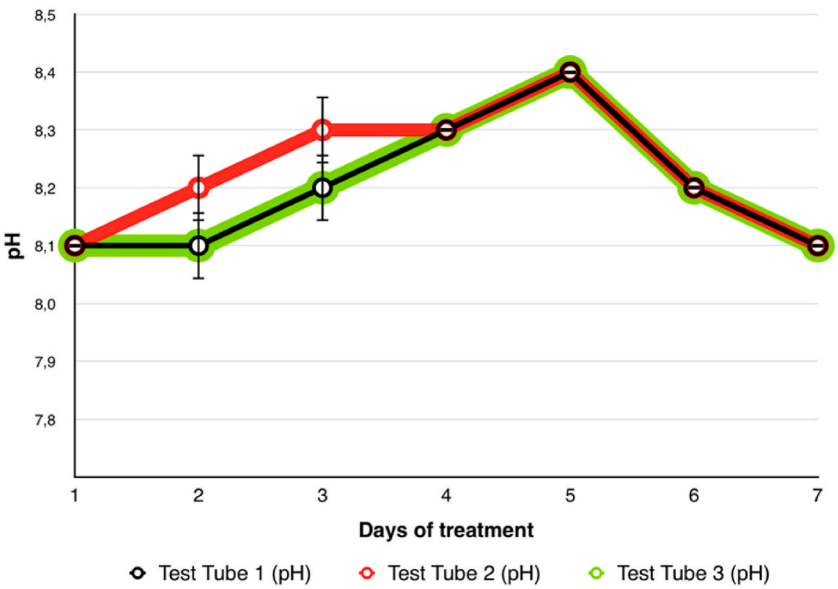

Fig. 3. Daily pH changes during the seven-day bioconsolidation treatment in three simultaneous pH tests tube analyses.

Samples	Initial Weight 1 (g)	Initial Weight 2 (g)	Initial Weight 3 (g)	Standard Deviation (g)	Mean Initial Weight (g)	Final Weight 1 (g)	Final Weight 2 (g)	Final Weight 3 (g)	Standard Deviation (g)	Mean Final Weight (g)	Increase (g)	Total Increase Standard Deviation (g)	% of Increase	Total % of Increase Standard Deviation
B-D2	5,0133	5,0131	5,0132	0,0001	5,0132	5,0326	5,0320	5,0337	0,0009	5,0328	0,0196		0,39	
B-D4	5,5762	5,5766	5,5770	0,0004	5,5766	5,6009	5,6006	5,6002	0,0004	5,6006	0,024		0,43	
B-D6	5,6245	5,6236	5,6237	0,0005	5,6239	5,6789	5,6772	5,6775	0,0009	5,6779	0,0539		0,96	
B-O1	9,2749	9,2747	9,2746	0,0002	9,2747	9,3035	9,3023	9,3021	0,0008	9,3026	0,0279		0,30	
B-O2	9,9985	9,9992	9,9988	0,0004	9,9988	10,0258	10,0256	10,0254	0,0002	10,0256	0,0268		0,27	
B-O3	10,8511	10,8514	10,8522	0,0006	10,8516	10,8878	10,8877	10,8875	0,0002	10,8877	0,0361		0,33	
B-SEM1	6,1055	6,1065	6,1065	0,0006	6,1062	6,1335	6,134	6,133	0,0005	6,1335	0,0273		0,45	
B-SEM2	7,3630	7,3637	7,3643	0,0007	7,3637	7,3974	7,3974	7,3972	0,0001	7,3973	0,0337		0,46	
B-SEM3	9,3886	9,3901	9,3905	0,0010	9,3897	9,4297	9,4288	9,4284	0,0007	9,4290	0,0392	0,0102	0,42	0,20
AVERAGES				0,0005					0,0005		0,0321		0,44	

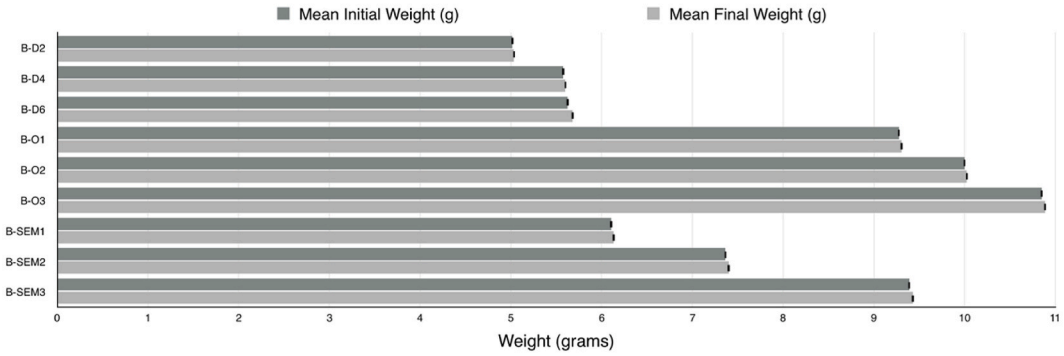

Fig. 4. Above: initial and final weight data of all samples and their statistics. Below: weight variations after *M. xanthus* treatment: initial and final mean weight for each sample.

upper area, highlighting in a light red band the samples that have changed significantly, exceeding tolerance index set in this research.

4.5. SEM analysis

Untreated control samples showed a compact structure in section, with poorly connected pores and some fissures (Fig. 6a). Surface appears slightly altered in section with no observable surface layers. (Fig. 6c). On surface (Fig. 6b) the characteristic fossil topography of calcium phosphate (hydroxyapatite), a basic component of bone remains, can be seen. Angular crystals can also be seen forming the surface (Fig. 6b). EDX analysis provides a spectrum that gives both on surface and inside the samples: carbon, phosphorus and calcium (Fig. 6d), attributable to typical hydroxyapatite laminar bone [83] and therefore to the original fossil carbonated calcium phosphate.

After treatment, induced calcium carbonate deposition, penetration depth and compositional and textural changes were observed in all samples. A surface layer of lighter chemical contrast was visible. This layer measures from 4 to 10 μm (minimum and maximum) but from 6 to 9 μm in most samples (in seven of the nine samples), with a mean of 7.44 μm and a standard deviation of 1.94 μm (Fig. 7). The newformed layer appears as a differentiated material (Figs. 7 and 8) which was not present in control samples (Fig. 6).

Two main spots were analysed by EDX: one on the surface (spot 1) and one inside the fossil (spot 2) for elemental comparison (Fig. 8a). EDX spectrum showed some differences between the surface layer (spot 1) and the internal area (spot 2). Although EDX is primarily a qualitative analysis, it is also semi-quantitative, thus it can be approximated than in the new surface layer (spot 1) more carbon and calcium, and traces of phosphorus were observed (Fig. 8b). However, in the internal area (spot 2), a spectrum similar to the controls was obtained (Figs. 8c and 6d).

In SEM sections, cast holes left by bacteria when coated with calcium carbonate were clearly observed. These holes were measured and results corresponded to *M. xanthus* regular size, between 1 and 3 μm in length and 0.5 μm in diameter (Fig. 8d).

New calcium carbonate did not penetrate into the substrate, remaining on the surface.

For surface textural study, calcified bacterial cells (cbc) were clearly observed (Fig. 9). Some of the rounded formations (cbc) were measured again and were coincident with *M. xanthus* regular dimensions (Fig. 9b). Some biofilm formation was detected in all cases.

No carbonate precipitation appeared in control treated samples, performed with uninoculated M-3P media.

4.6. Powder X-ray diffraction analysis

Untreated fossil showed the presence of hydroxyapatite and calcite (Fig. 10d) as would be expected in a highly carbonated fossil. Hydroxyapatite was found in higher proportion than calcite, the relative mass fraction being 56:44.

By contrast, although bioconsolidated layers also presented calcite and hydroxyapatite (Fig. 10a–c), coinciding with EDX analysis,

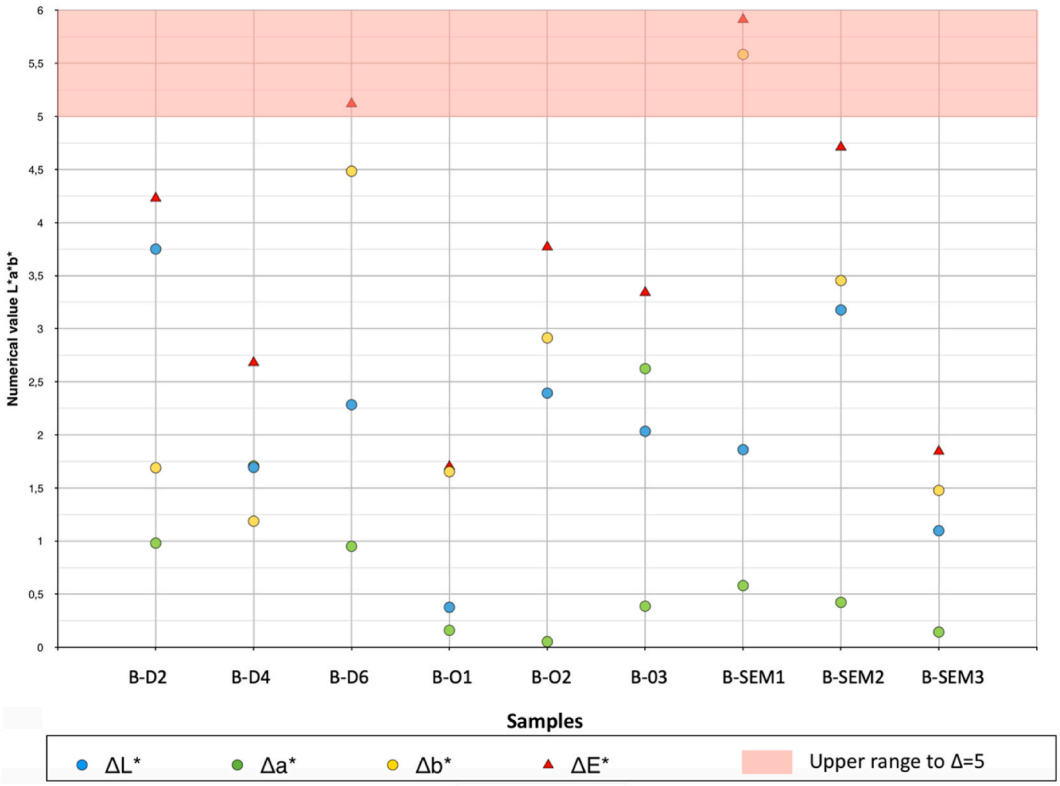

Fig. 5. Colour variations after *M. xanthus* treatment between average L*a*b* data: ΔL* Δa* Δb* ΔE* and ΔE*. (For interpretation of the references to colour in this figure legend, the reader is referred to the Web version of this article.)

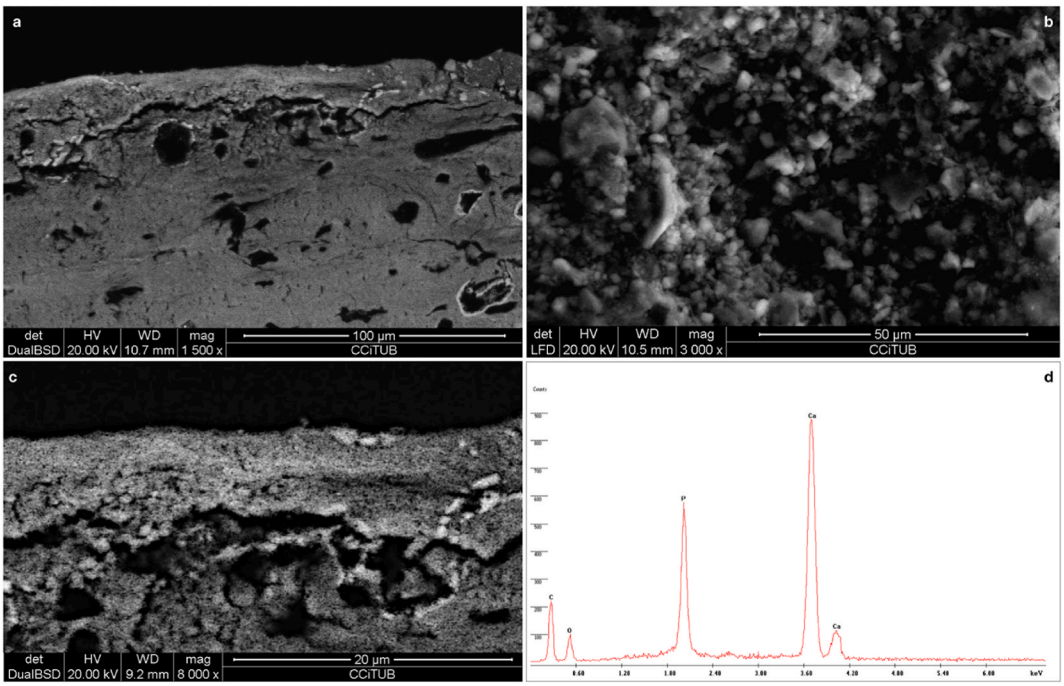

Fig. 6. SEM-BEI and SEM-SEI photomicrographs and EDX spectrum of control untreated samples. (a) Control C1 sample surface section at 1500x. (b) Control C2 sample surface image at 3000x. (c) Control C1 sample surface section at 8000x. (d) EDX surface spectrum corresponding to control C2 sample: carbon, phosphorus and calcium.

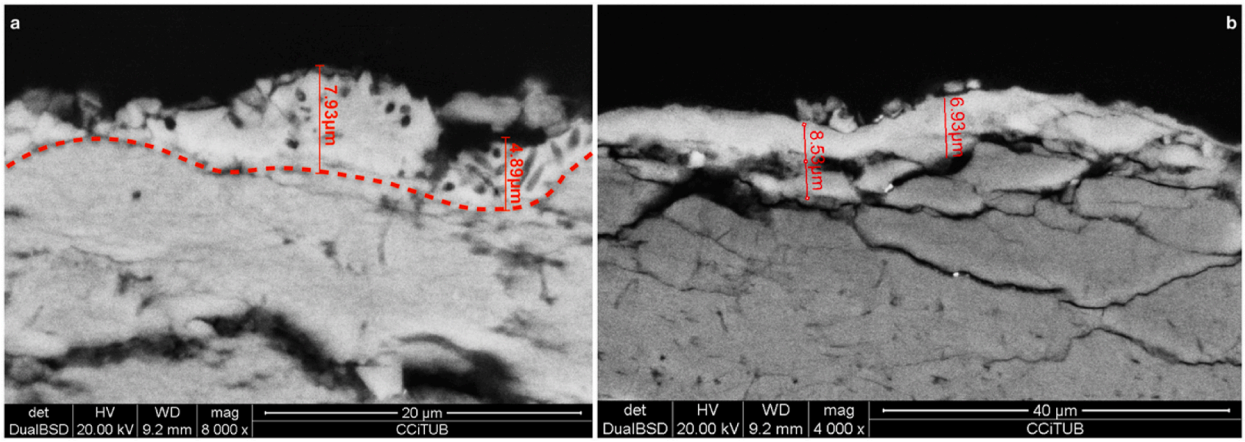

Fig. 7. SEM-BEI photomicrographs of *M. xanthus* inoculated sample B-SEM2 and B-D6. (a) Sample B-SEM2 surface section at 8000x. In red, thickness measurements of the newformed layer. (b). Sample B-D6 surface section at 4000x. In red, thickness measurements of the newformed layer. (For interpretation of the references to colour in this figure legend, the reader is referred to the Web version of this article.)

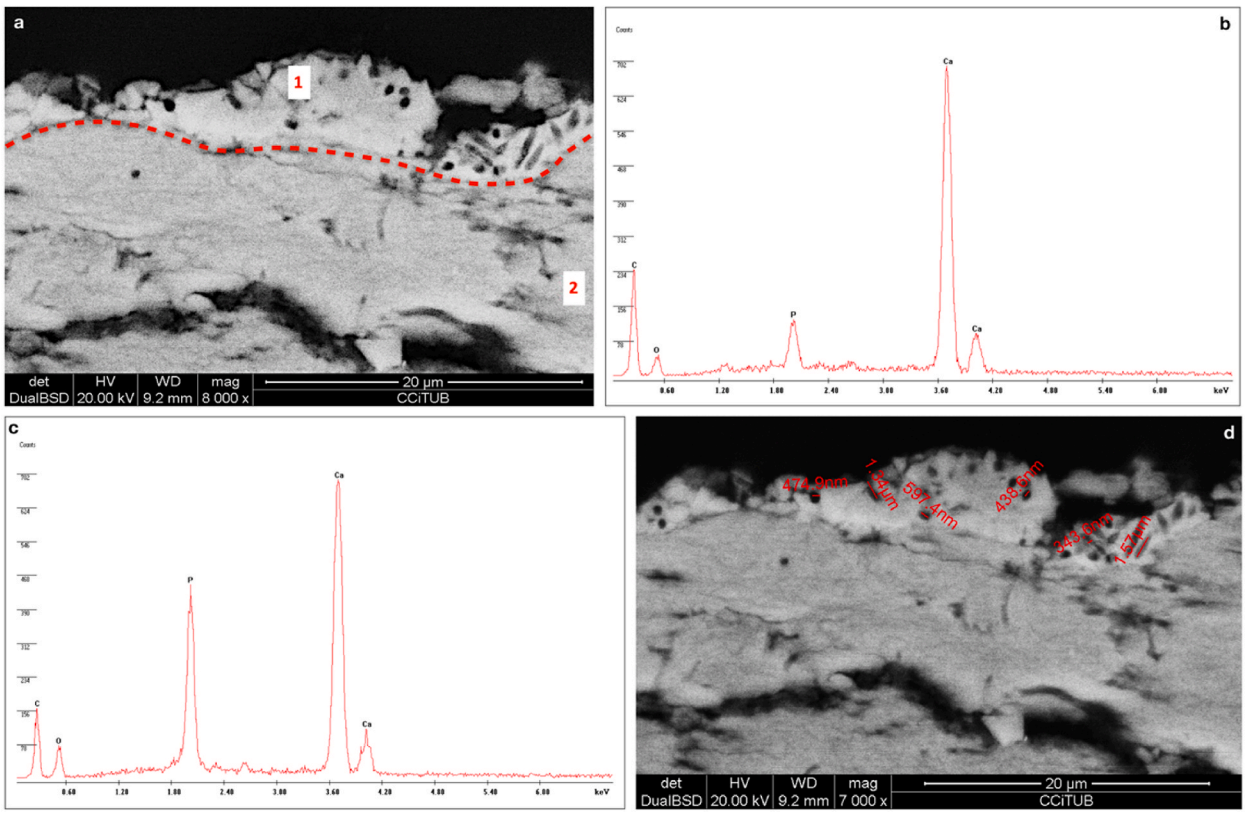

Fig. 8. SEM-BEI photomicrographs and EDX spectrum of *M. xanthus* inoculated sample B-SEM2. (a) Sample surface section. The border between the newly formed layer and the original fossil surface is marked by a red line. (b) EDX spot 1 spectrum corresponding to the newly formed layer. (c) EDX spot 2 spectrum corresponding to fossil internal area: carbon, phosphorus and calcium comparable to control samples. (d) Sample surface section. Holes left by bacteria when coated with calcium carbonate. These cast spaces corresponded to *M. xanthus* regular size, between 1 and 3 µm in length and 0.5 µm in diameter. Over the new layer, with differentiated chemical contrast, small biofilm residues can be observed. (For interpretation of the references to colour in this figure legend, the reader is referred to the Web version of this article.)

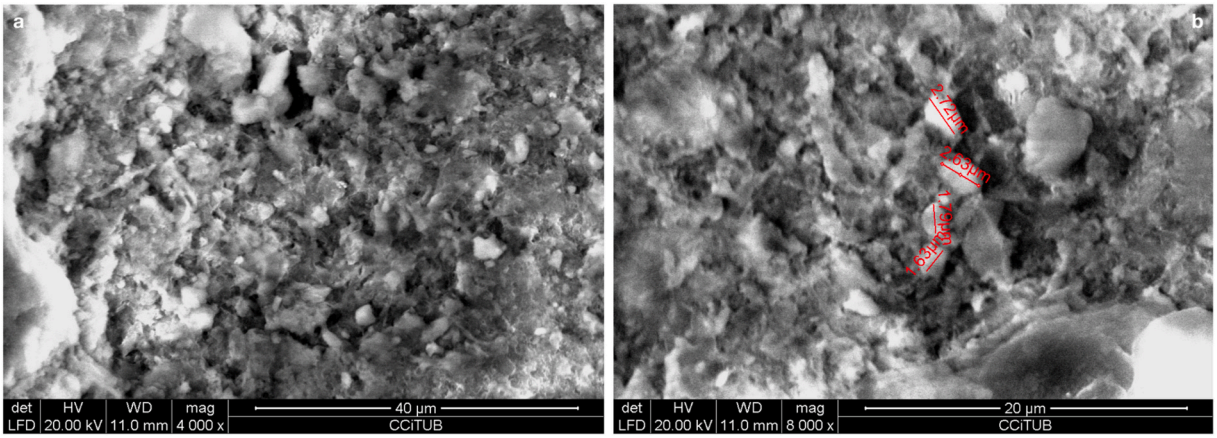

Fig. 9. SEM-SEI photomicrographs of *M. xanthus* inoculated sample B–O1 and B–O3. (a) Sample B–O1 surface image. Calcified bacterial cells (cbc). (b) Sample B–O3 surface image. Calcified bacterial cells (cbc) measured.

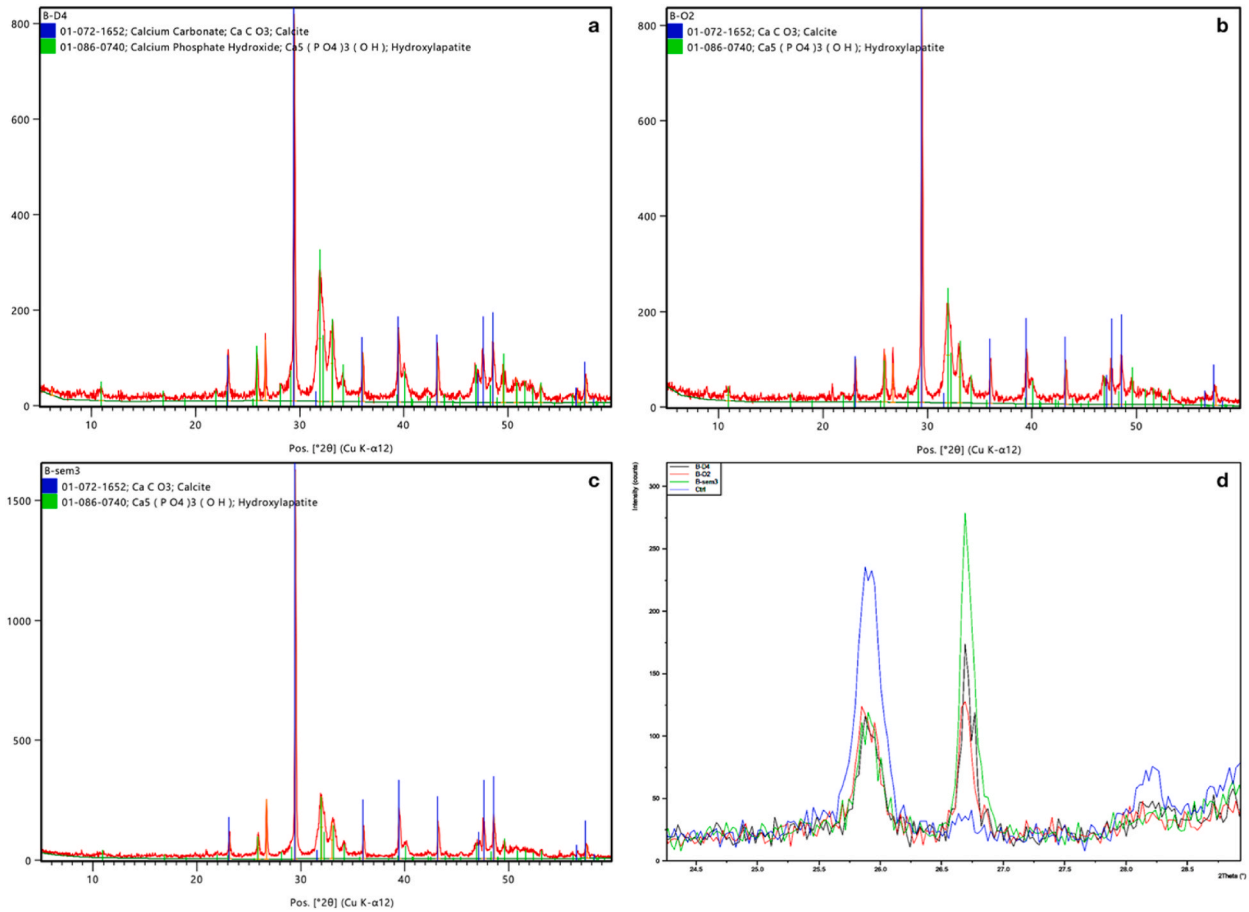

Fig. 10. XRD diffractograms of samples B-D4 (a), B–O2 (b) and B-SEM3 (c). Combined diffractogram of all samples compared to the control (d).

they showed a higher proportion of calcite, the relative mass fraction being 42:58 (58 is the average for the three samples, standard deviation: 10%) (Fig. 10d).

4.7. Drop absorption analysis

During the nine measurements performed on the nine samples prior to consolidation, a standard deviation from 0.21 to 0.60 s and a standard deviation mean of 0.39 s was obtained. After consolidation, a standard deviation from 0.25 to 1.14 s and a standard deviation mean of 0.46 s was recorded.

Drop absorption time increased in all cases (Fig. 11). After treatment, absorption times performed an augmentation of between 160.14 and 397.38 s with an average of 274,07 s and a standard deviation of 75.55 s. Consequently, original absorption times were multiplied from 7.35 times to 37.97 times with an average of 13.22 times and a standard deviation of 9.66.

4.8. Vickers microindentation hardness analysis

Surface hardness increased significantly compared to control values (Fig. 12). Original control hardness showed average results of 0.016 kg/mm^2. After treatment, values averaged 0.028 kg/mm^2, which is an increase of 75%.

On bioconsolidated samples, standard deviations range from 0,002 to a maximum of 0,012 kg/mm^2 with a standard deviation average of 0,007 kg/mm^2.

4.9. Disaggregation tape test

Fossil surface disaggregation was analysed before and after treatment. Significant variations were observed in the weight of detached fossil particles before and after bioconsolidation. After treatment, a large decrease in surface disaggregation was seen (Fig. 13). Samples initially released a considerable number of particles, ranging from dust particles to small fragments of 0.5 mm, but in the final tests, fossil surface was very cohesive, with no fragments detached and almost no loose particles.

The weight of detached particles decreased in all cases (Fig. 13). Tape test samples performed weight reduction around 0.0018 and 0.0095 g, with an average of 0.005 g and a standard deviation of 0.0022 g. In percentage terms, that means a decrease of between 61.04% and 100%, with a total arithmetic average of 75.24% and a standard deviation of 13.83%.

5. Discussion

In this study *M. xanthus* induced calcium carbonate precipitation on fossils as evidenced in SEM and XRD analysis (Figs. 7 and 8). Compositional and textural changes were observed in all samples, in particular a surface layer of lighter chemical contrast was visible (Fig. 7).

Other signs indicating calcium carbonate precipitation have been observed, such as pH increase during the experiments. As explained in section 2, *M. xanthus* metabolic activity involved in MICP is closely related to pH. This could be observed in the pH ranges during the first five days of fossil consolidation treatment: between 8 and 8.4 and then a decay to 8.1 the last days [section 4.2, Fig. 3]. According to Rodríguez-Navarro et al. [24], it was proven that pH decrease starts when calcium carbonate precipitation rate is nearing its maximum value. Thus, pH decrease due to the precipitation of calcium carbonate [50].

As observed with EDX analysis (Fig. 8) the newly formed layer was very similar in composition to the original fossil. A calcite organic-inorganic cement compositionally similar to that formed in fossil remains over millennia has been obtained. Hydroxyapatite was also detected in low relative proportions to the original fossil. Bacterial consolidation replicates microbial permineralization during the fossilisation process. Indeed, most fossils consist of biomineralized remains [28]. In this respect, this bioconsolidation experiment was highly compatible with the original fossil.

As observed in PXRD, newly formed layers consist of calcite and hydroxyapatite, similar to the original untreated fossil, but with a higher presence of calcite and a lower presence of hydroxyapatite. Significant amounts of hydroxyapatite in the bacterially created layer can be explained in three ways. Firstly because of the difficulty of removing only the consolidated part in the irregular samples during PXRD sampling. Despite this, a decreasing trend in hydroxyapatite was observed and an increase in calcite, which was also noticeable in the EDX element identification (Figs. 6 and 8). On the other hand, the presence of small amounts of hydroxyapatite in this new layer may also be explained for the pulverulence of the samples surface prior to consolidation. The new layer bound the surface pulverulence as shown in the disaggregation tape test [section 4.9]. Finally, the presence of small amounts of hydroxyapatite created by *M. xanthus* bioconsolidation was also documented in the literature [24] and may also be related to the interaction of bacterial metabolic activity with the fossil surface.

Regarding bacterial monitoring [section 4.1], results demonstrated massive presence of *M. xanthus* in all samples during treatment. In terms of contaminations, no other bacteria grown on samples was found, so the treatment proved to be controllable and safe.

After treatment, ATP assay confirmed no live bacteria remains on fossil surfaces. In this case, after rinsing and drying, ATP monitoring reported 0 RLU data. The same results were repeated for the following 10 days and 12 weeks, so *M. xanthus* treatment proved to be totally safe. Thus, it was demonstrated that treatment can be stopped at any time by rinsing and drying. Bacteria died and therefore the treatment is consistent.

Both the composition of precipitated calcite and the safety of using a single type of bacteria, eradicated after rinsing and drying, make the treatment very stable over time. Inorganic materials are very resistant to ageing and deterioration in contrast to polymeric

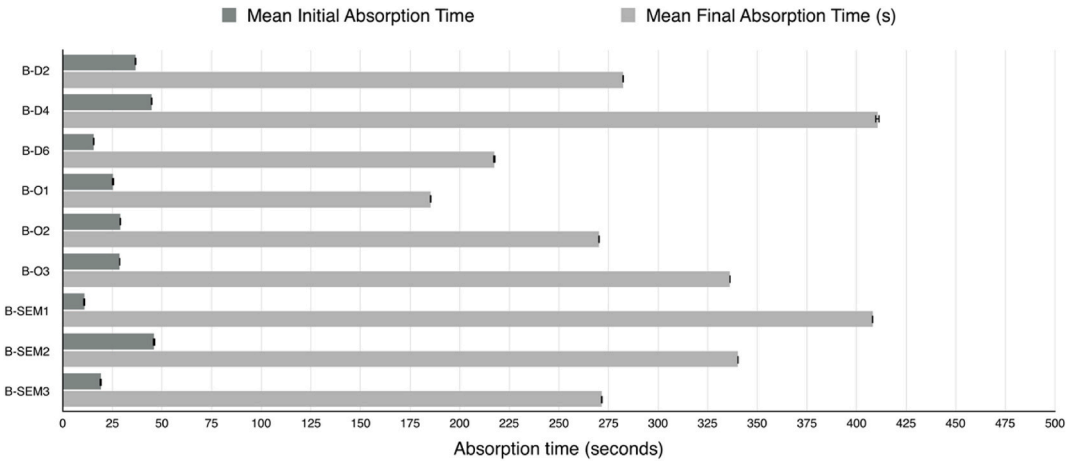

Fig. 11. Absorption time variations after *M. xanthus* treatment: initial and final mean absorption time for each sample.

Samples	HV 1 (kg/mm²)	HV 2 (kg/mm²)	HV 3 (kg/mm²)	HV 4 (kg/mm²)	HV 5 (kg/mm²)	Standard Deviation	Total Standard Deviation Mean	HV mean	Total HV mean
Control 1	0,017	0,021	0,031	0,017	0,015	0,006		0,020	
Control 2	0,014	0,009	0,011	0,008	0,012	0,002		0,011	
Control 3	0,016	0,017	0,018	0,020	0,014	0,002		0,017	
Control 4	0,021	0,011	0,016	0,013	0,012	0,004	**0,004**	0,015	**0,016**
B-D2	0,010	0,018	0,016	0,012	0,009	0,004		0,013	
B-D4	0,022	0,018	0,025	0,028	0,033	0,006		0,025	
B-D6	0,055	0,043	0,045	0,053	0,040	0,006		0,047	
B-O1	0,026	0,021	0,025	0,023	0,030	0,003		0,025	
B-O2	0,045	0,023	0,05	0,023	0,035	0,012		0,035	
B-O3	0,021	0,010	0,038	0,031	0,038	0,012		0,028	
B-SEM1	0,038	0,051	0,018	0,027	0,037	0,012		0,034	
B-SEM2	0,026	0,022	0,026	0,023	0,025	0,002		0,024	
B-SEM3	0,025	0,022	0,026	0,024	0,023	0,002	**0,007**	0,024	**0,028**

Fig. 12. Vickers microindentation hardness analysis: original (control untreated samples) and after bioconsolidation treatment.

Samples	Initial Weight (g)	Final Weight (g)	Decrease (g)	Total Decrease Standard Deviation (g)	% of Decrease	Total % of Decrease Standard Deviation
B-D2	0,0049	0	0,0049		100,00	
B-D4	0,0025	0,0007	0,0018		72,00	
B-D6	0,007	0,0006	0,0064		91,43	
B-O1	0,005	0,0015	0,0035		70,00	
B-O2	0,0077	0,003	0,0047		61,04	
B-O3	0,0171	0,0076	0,0095		55,56	
B-SEM1	0,0045	0,001	0,0035		77,78	
B-SEM2	0,0077	0,0022	0,0055		71,43	
B-SEM3	0,0068	0,0015	0,0053	0,0022	77,94	13,83
AVERAGES	0,0070	0,0020	0,005		75,24	

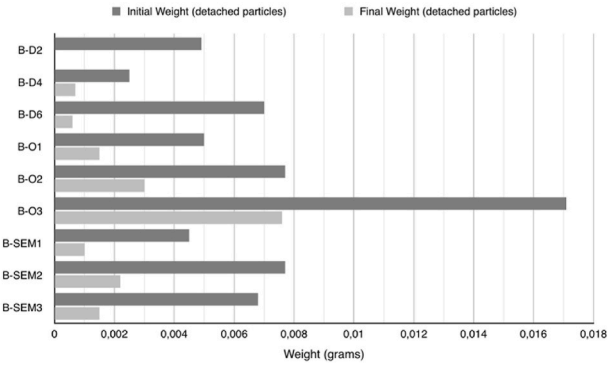

Fig. 13. Left: Tape test initial and final detached weight data and their statistics. Right: Detached particles weight variations after *M. xanthus* treatment: initial and final detached particles weight for each sample.

resins usually used. Furthermore, it was demonstrated that bacterially induced calcite exhibited greater resistance to dissolution (against water and acids) than inorganically precipitated calcite [24,84].

According to SEM analysis, *M. xanthus* calcium carbonate cement has not penetrated into the substrate (Figs. 7 and 8). The newly formed layer has been developed just on top of the fossil surface with a 6–9 μm thickness (Fig. 7). Null penetration may be due to fossil intrinsic characteristics. This specimen has low cortical porosity and very small pore size, smaller than bacteria (Fig. 6). Therefore, bacteria cannot penetrate through the substrate. By contrast, some studies have shown that bioconsolidation by *M. xanthus* penetrated

up to 1 mm, and with a surface layer of 10–50 μm, but this is referred to on porous limestone samples [24]. However, as the treated fossil only presented superficial disaggregation but not deep disintegration, the treatment was effective and adequate.

In surface textural analysis, calcified bacterial cells (cbc) were clearly observed corresponding to the nucleation areas for mineral deposition (Fig. 9). Cbc and cast holes had a shape and size ascribable to *M. xanthus* (Fig. 9b). PXRD analysis combined with EDX allows to state that the layer created on bioconsolidated samples consists of calcite binding the disintegrated fossil particles together.

Although M-3P culture media considerably reduces EPS biofilm formation according to Rodríguez-Navarro et al. [24] some biofilm formation was detected in all cases (Fig. 8). According to González-Muñoz [53], non-massive EPS biofilm can have a positive effect on surface cohesion due to their binding action as long as they do not block the pores [53].

In terms of treatment's consolidation effects, this methodology provides encouraging hardening and cohesion data (Figs. 12 and 13). Regarding cohesion, a large decrease in surface disaggregation was observed (Fig. 13). Most of the disaggregated surface particles were bound together by the formation of a calcium carbonate surface layer (6–9 μm). Fossil surface became very cohesive, with no fragments detached and almost no loose particles. In percentage terms, that means an average decrease of 75.24%.

These are the main factors to be assessed in fossil surface consolidation. Improvements in hardness and cohesion are generally necessary to preserve the morphology and integrity of decayed fossils. In this respect, this treatment proves to be most appropriate. However, to further assess its suitability, it is necessary to consider the characteristics of the fossil that should not be altered by the treatment.

Consolidating treatments should not cause material incompatibility, pore clogging, significant aesthetic changes, substantial weight changes, noticeable physicochemical alterations or film surface formation. In this research, although changes in porosity and absorption behaviour were monitored (Fig. 11), no total blockage occurred in any sample. The layer formed was porous and heterogeneous, thus allowing permeability (Figs. 7 and 8).

Concerning colour and brightness changes, these were minimal and imperceptible (Fig. 5) with values that cannot be seen by the human eye ($\Delta E < 5$) [80–82]. Only two samples slightly exceed the tolerance index set in this research, showing an almost imperceptible yellowing. It is possible to say that *M. xanthus* bioconsolidation made no or hardly any alteration to the aesthetic appearance. This can be attributed to the fact that the newformed calcium carbonate layer is very thin (6–9 μm) and transparent.

With regard to weight changes, samples performed some gain with an average of 0.44% (Fig. 4). It is a slight and natural increase due to the thin calcium carbonate layer formation. In any case it isn't an increase that could endanger the integrity of the fossil or lead to pore clogging [24].

Although small pH variations occurred during treatment, because of metabolic alkalinisation and calcium carbonate precipitation (Fig. 3), fossil pH remained stable after rinsing and drying. At the end of the experiment pH was identical to the original fossil pH: 8. This is a positive aspect considering that heritage treatments must have adequate pH and conductivity, slightly alkaline pH and isotonic conductivity similar to the original fossil to prevent calcium carbonate and calcium phosphate solubility damage [85,86].

Conductivity increased in all cases (Fig. 2) but this is to be expected considering that a calcium carbonate organic-inorganic layer has been created (and by the culture media addition). Even with this increase, conductivity data were still standard and close to isotonicity according to current conservation-restoration criteria [85,86]. In addition, calcium carbonate is a fairly insoluble salt, (pK_{sp} 8.54) so it will not migrate or create cyclic salt dissolution-recrystallisation problems.

6. Conclusions

This research proves that calcium carbonate precipitation induced by MICP has a positive effect on the protection of carbonate fossil heritage. Consequently, it is an effective consolidation treatment for decayed carbonate fossils and highly compatible with the substrate, providing good hardening and cohesion.

Furthermore, treatment does not generate pore clogging, noticeable aesthetic changes, significant weight increase, chemical alteration or film surface formation: the main properties that consolidation treatments should not alter.

This methodology outperforms traditional polymeric treatments because it reaches the compatibility, minimum intervention, retractability and stability of conservation criteria.

Regarding its applicability, this methodology is not as simple as applying a polymeric resin by brush. It requires about 7 days of treatment and the conservator-restorer needs some training in microbiology, otherwise, a microbiologist or laboratory support may be required. Even so, the advantages far outweigh these minor difficulties and treatment is simple and quick. On the other hand, immediate bacterial monitoring systems such as ATP luminometer analysis make interventions easy even on site. In addition, *M. xanthus* calcium carbonate precipitation is a non-toxic and environmentally friendly consolidation treatment.

For all these reasons, this research represents a new approach to consolidation alternatives in the palaeontological conservation field. Until now, bioconsolidation research has focused on stone and wall paintings, but never on paleontological and fossil heritage. Now, *M. xanthus* induced calcium carbonate precipitation is proposed as an innovative strategy on palaeontological heritage conservation.

However, more research to develop this new conservation treatment is needed. Future research should be focused on higher porosity fossil supports to test if higher penetration is possible as referred to in literature. On the other hand, new research lines could involve the use of fossil endogenous bacteria to achieve an even more compatible treatment. And to advance in this proposal, bacterial consolidation should also be tested on other kinds of fossil specimens, non-fossilised bone and ivory remains and objects.

Author contribution statement

Silvia Marín-Ortega: Conceived and designed the experiments; Performed the experiments; Analysed and interpreted the data; Contributed reagents, materials, analysis tools or data; Wrote the paper.

M. Àngels Calvo i Torras: Conceived and designed the experiments; Performed the experiments; Contributed reagents, materials, analysis tools or data.

Manuel Ángel Iglesias-Campos: Conceived and designed the experiments; Performed the experiments; Contributed reagents, materials, analysis tools or data; Wrote the paper.

Data availability statement

Data included in article/supp. material/referenced in article.

Declaration of competing interest

The authors declare that they have no known competing financial interests or personal relationships that could have appeared to influence the work reported in this paper

Acknowledgements

We thank Leonardo Arosemena, Research Support Technician in VO-279 Laboratory (Applied and Environmental Microbiology Research Group, Universitat Autònoma de Barcelona, Faculty of Veterinary Medicine). Thanks also to Sandra Val and CRIP Institution for providing fossil sample fragments for this research. Also, we thank KBYO Biological for providing M-3P culture media.

References

[1] F. Petrie, Methods & Aims in Archaeology, British Library Cataloguing-in-Publication Data, London, 1904. ISBN 9780344362750.
[2] F. Rathgen, The preservation of antiquities, in: A Handbook for Curators, Cambridge University Press, Cambridge, 1905. ISBN 9781107635258.
[3] F.M.P. Howie, Materials used for conserving fossil specimens since 1930: a review, Stud. Conserv. 29 (1) (1984) 92–97, https://doi.org/10.1179/sic.1984.29.Supplement-1.92.
[4] L. Lazzarini, M. Laurenzi, Il restauro della pietra, Cedam Casa Editrice, Milan, 1986. ISBN 9788859805434.
[5] L. Borgioli, Polimeri di sintesi per la conservazione della pietra, Collana i Talenti. Il Prato, Saonara, 2006. ISBN 9788887243383.
[6] C. Horie, Materials for Conservation: Organic Consolidants, Adhesives, and Coatings, Butterworth-Heinemann, Oxford, London, 1987. ISBN 9780750608817.
[7] J.M. Cronyn, The Elements of Archaeological Conservation, Routledge, London, 1990. ISBN 9780415012072.
[8] C. Pedeli, S. Pulga, Pratiche conservative sullo scavo archeologico, Edicione del Giglio, Florence, 2002. ISBN 9788878145009.
[9] A.E. Rixon, Fossil Animal Remains: Their Preparation and Conservation, Athlone Press, London, 1976. ISBN 9780485120288.
[10] J.S. Johnson, Consolidation of archaeological bone: a conservation perspective, J. Field Archaeol. 21 (1994) 221–233, https://doi.org/10.2307/529866.
[11] L.A. Kres, N.C. Lovell, A comparison of consolidants for archaeological bone, J. Field Archaeol. 22 (1995) 508–515, https://doi.org/10.1179/009346995791974134.
[12] D. De Rossi, S. De Gruchy, N.C. Lovell, A comparative experiment in the consolidation of cremated bone, Int. J. Osteoarchaeol. 14 (2004) 104–111, https://doi.org/10.1002/oa.715.
[13] P. Leiggi, P. May, Vertebrate Paleontological Techniques, Cambridge University Press, Cambridge, 2005. ISBN 9780521459006.
[14] L. López-Polín, J.M. Bermúdez De Castro, E. Carbonell, The preparation and conservation treatments of the human fossils from Lower Pleistocene unit TD6 (Gran Dolina site, Atapuerca). The 2003-2009 record, Quat. Int. 433 (2017) 251–262, https://doi.org/10.1016/j.quaint.2015.09.036.
[15] S.P. Koob, in: P. Smith, G. Thomson, N.S. Brommelle, E.M. Pye (Eds.), The Consolidation of Archaeological Bone, Adhesives and Consolidants. Preprints of of the Contributions to the Paris Congress, 2-8 September, International Institute for Conservation of Historic and Artistic Works, London, 1984, pp. 98–102.
[16] J.A. Eklund, M.G. Thomas, Assessing the effects of conservation treatments on short sequences of DNA in vitro, J. Archaeol. Sci. 37 (2010) 2831–2841, https://doi.org/10.1016/j.jas.2010.06.019.
[17] L. López-Polín, Possible interferences of some conservation treatments with subsequent studies on fossil bones: a conservator's overview, Quat. Int. 275 (2012) 120–127, https://doi.org/10.1016/j.quaint.2011.07.039.
[18] J. Ashley-Smith, Adhesives and Coatings. The Science for Conservators Series, in: Conservation Unit Museums and Galleries Commission, ume 3, Routledge, Taylor & Francis Group, London & New York, 1992. ISBN 9780415071635.
[19] P. Tiano, in: L. Becagli, S. Metaldi (Eds.), Precipitazione bioindotta di calcite per il rinforzo delle pietre monumentali, I batteri nel restauro. I principi, l'esperienza di laboratorio e i casi studio applicati dalla biopulitura al bioconsolidamento, Il Prato. Centro Europeo per i Meisteri del Patrimonio, Thiene, 2013, pp. 241–272.
[20] F. Jroundi, M.T. González-Muñoz, A. García-Bueno, C. Rodríguez-Navarro, Consolidation of archaeological gypsum plaster by bacterial biomineralization of calcium carbonate, Acta Biomater. 10 (2014) 3844–3854, https://doi.org/10.1016/j.actbio.2014.03.007.
[21] A. North, M. Balonis, I. Kakoulli, Biomimetic hydroxyapatite as a new consolidating agent for archaeological bone, Stud. Conserv. 61 (3) (2016) 146–161, https://doi.org/10.1179/2047058415Y.0000000020.
[22] A. Barberà, S. Marín-Ortega, P. Rovira, in: E. Vieira, P. Moreira, M. Pintado, A. Macchia (Eds.), The Removal of Paraloid® Coatings with Aqueous Based Formulations. Practical Case in Frescoes from Els Munts Roman Villa (Catalonia), Proceedings of 3rd Green Conservation Conference. Universidade Católica Portuguesa, vol. 10, ECR - Estudos de Conservação e Restauro, 2019, pp. 67–83, https://doi.org/10.34632/ecr.2019.9580.
[23] I. Reiche, C. Vignaud, M. Menu, The crystallinity of ancient bone and dentine: new insights by transmission electron microscopy, Archaeometry 44 (3) (2002) 447–459, https://doi.org/10.1111/1475-4754.00077.
[24] C. Rodríguez-Navarro, M. Rodríguez-Gallego, K.B. Chekroun, M.T. González-Muñoz, Conservation of ornamental stone by *Myxococcus xanthus* induced carbonate biomineralization, Appl. Environ. Microbiol. 69 (4) (2003) 2182–2193, https://doi.org/10.1128/AEM.69.4.2182-2193.2003.
[25] C. Bisulca, L. Kronthal, A. Davidson, Consolidation of fragile fossil bone from Ukhaa Tolgod, Mongolia (late cretaceous) with CONSERVARE OH100, J. Am. Inst. Conserv. 48 (2009) 37–50, https://doi.org/10.1179/019713609804528098.
[26] C.M. Nielsen-Marsh, R.E.M. Hedges, Patterns of diagenesis in bone I: the effects of site environments, J. Archaeol. Sci. 27 (12) (2000) 1139–1150, https://doi.org/10.1006/jasc.1999.0537.

[27] J. Sagemann, S.J. Bale, D.E.G. Briggs, R.J. Parkes, Controls on the formation of authigenic minerals in association with decaying organic matter: an experimental approach, Geochem. Cosmochim. Acta 63 (7/8) (1999) 1083–1095, https://doi.org/10.1016/S0016-7037(99)00087-3.

[28] D.E.G. Briggs, The role of decay and mineralization in the preservation of soft-bodied fossils, Annu. Rev. Earth Planet Sci. 31 (2003) 275–301, https://doi.org/10.1146/annurev.earth.31.100901.144746.

[29] J.E. Peterson, M.E. Lenczewski, R.P. Scherer, Influence of microbial biofilms on the preservation of primary soft tissue in fossil and extant archosaurs, PLoS One 5 (10) (2010), e13334, https://doi.org/10.1371/journal.pone.0013334.

[30] C. Zabini, J.D. Schiffbauer, S. Xiao, M. Kowalewski, Biomineralization, taphonomy, and diagenesis of Paleozoic lingulide brachiopod shells preserved in silicified mudstone concretions, Palaeogeogr. Palaeoclimatol. Palaeoecol. 326–328 (2012) 118–127, https://doi.org/10.1016/j.palaeo.2012.02.010.

[31] P.A. Allison, The role of anoxia in the decay and mineralization of proteinaceous macro-fossils, Paleobiology 14–2 (1988) 139–154, https://doi.org/10.1017/S009483730001188X.

[32] G.L. Osés, S. Petri, C.G. Voltani, G.M.E.M. Prado, D. Galante, M.A. Rizzutto, I.D. Rudnitzki, E.P. Da Silva, F. Rodrigues, E.C. Rangel, P.A. Sucerquia, M.L.A. F. Pacheco, Deciphering pyritization-kerogenization gradient for fish soft-tissue preservation, Sci. Rep. (Nature) 7 (2017) 1468–1482, https://doi.org/10.1038/s41598-017-01563-0.

[33] A.M. Child, Microbial taphonomy of archaeological, Bone. Stud. Conserv. 40 (1) (1995) 19–30, https://doi.org/10.1179/sic.1995.40.1.19.

[34] R.A. Robinson, Treatise on Invertebrate Paleontology. Part A -Introduction- Fossilization (Taphonomy), Biogeography, and Biostratigraphy, Geological Society of America Incorporated, Kansas, 1979. ISBN 9780813730011.

[35] I. Natali, P. Tempesti, E. Carretti, M. Potenza, S. Sansoni, P. Baglioni, L. Dei, Aragonite crystals grown on bones by reaction of CO2 with nanostructured Ca(OH)2 in the presence of collagen. Implications in archaeology and paleontology, Langmuir 30 (2) (2014) 660–668, https://doi.org/10.1021/la404085v.

[36] E. Boquet, A. Boronat, A. Ramos-Cormenzana, Production of calcite (calcium carbonate) crystals by soil bacteria is a general phenomenon, Nature 246 (1973) 527–529, https://doi.org/10.1038/246527A0.

[37] J.M. Adolphe, J.F. Loubière, J. Paradas, F. Soleilhavoup, Procédé de traitement biologique d'une surface artificielle, 1990. European patent 90400G97.0.

[38] G. Orial, S. Castanier, G. Le Métayer-Levrel, J.F. Loubiere, in: H. Ktoishi, T. Arai, K. Yamano (Eds.), The Biomineralization: a New Process to Protect Calcareous Stone Applied to Historic Monuments, Proceedings of the 2nd International Conference on Biodeterioration of Cultural Property, International Communications Specialists, Tokyo, 1993, pp. 98–116.

[39] G. Le Métayer-Levrel, S. Castanier, G. Orial, J.F. Loubière, J.P. Perthuisot, Applications of bacterial carbonatogenesis to the protection and regeneration of limestones in buildings and historic patrimony, Sediment. Geol. 126 (1999) 25–34, https://doi.org/10.1016/S0037-0738(99)00029-9.

[40] P. Tiano, L. Biagiotti, G. Mastromei, Bacterially bio-mediated calcite precipitation for monumental stones conservation: methods of evaluation, J. Microbiol. Methods 36 (1999) 139–145, https://doi.org/10.1016/S0167-7012(99)00019-6.

[41] S. Castanier, G. Le Métayer-Levrel, G. Orial, J.F. Loubière, J.P. Perthuisot, in: O. Ciferri, P. Tiano, G. Mastromei (Eds.), Bacterial Carbonatogenesis and Applications to Preservation and Restoration of Historic Property, Of Microbes and Art: the Role of Microbial Communities in the Degradation and Protection of Cultural Heritage, Plenum, New York, 2000, pp. 201–216, https://doi.org/10.1007/978-1-4615-4239-1_14.

[42] F. Jroundi, M. Schiro, E. Ruiz-Agudo, K. Elert, I. Martín-Sánchez, M.T. González-Muñoz, C. Rodríguez-Navarro, Protection and consolidation of stone heritage by self-inoculation with indigenous carbonatogenic bacterial communities, Nat. Commun. 8 (1) (2017) 279–291, https://doi.org/10.1038/s41467-017-00372-3.

[43] F. Jroundi, C. Rodríguez-Navarro, A. García Bueno, V. Medina-Flórez, M.T. González-Muñoz, in: A.M. López, F. Collado, V. Medina, T. Espejo, A. García (Eds.), Consolidación de materiales arqueológicos procedentes del Alcázar de Guadalajara mediante carbonatogénesis bacteriana, Proceedings of the XVIII Congreso Internacional de Conservación y Restauración en Bienes Culturales, Universidad de Granada, Granada, 2011, pp. 125–127. ISBN 978-84-338-5339-4.

[44] A.I. Calero-Castillo, T. López-Martínez, A. García-Bueno, M.T. González-Muñoz, V.J. Medina-Flórez, Ensayos de consolidación en los revestimientos murales del Conjunto Arqueológico de Cástulo (Linares, Jaén), Ge-conservación 10 (2016) 31–43, https://doi.org/10.37558/gec.v10i0.346.

[45] C. Buczynski, H.S. Chafetz, Habit of bacterially induced precipitates of calcium carbonate and the influence of medium viscosity on mineralogy, J. Sediment. Petrol. 61 (1991) 226–233, https://doi.org/10.1306/D42676DB-2B26-11D7-8648000102C1865D.

[46] R. Folk, SEM imaging of bacteria and nannobacteria in carbonate sediments and rocks, J. Sediment. Petrol. 63 (1993) 990–999, https://doi.org/10.1306/D4267C67-2B26-11D7-8648000102C1865D.

[47] S. Castanier, G. Le Métayer-Levrel, J.P. Perthuisot, Ca-carbonates precipitation and limestone genesis. The microbiologist point of view, Sediment. Geol. 126 (1999) 9–23, https://doi.org/10.1016/S0037-0738(99)00028-7.

[48] D.E.G. Briggs, A.J. Kear, Fossilization of soft tissue in the laboratory, Science 259 (1993) 1439–1442, https://doi.org/10.1126/science.259.5100.1439.

[49] C. Rodríguez-Navarro, C. Jiménez-López, A. Rodríguez-Navarro, M.T. González-Muñoz, M. Rodríguez-Gallego, Bacterially mediated mineralization of vaterite, Geochimica 71 (2007) 1197–1213, https://doi.org/10.1016/j.gca.2006.11.031.

[50] C. Jiménez-López, C. Rodríguez-Navarro, G. Piñar, F.J. Carrillo-Rosúa, M. Rodríguez-Gallego, M.T. González-Muñoz, Consolidation of degraded ornamental porous limestone stone by calcium carbonate precipitation induced by the microbiota inhabiting the stone, Chemosphere 68 (2007) 1929–1936, https://doi.org/10.1016/j.chemosphere.2007.02.044.

[51] C. Jiménez-López, F. Jroundi, C. Pascolini, C. Rodríguez-Navarro, G. Piñar-Larrubia, M. Rodríguez-Gallego, M.T. González-Muñoz, Consolidation of quarry calcarenite by calcium carbonate precipitation induced by bacteria activated among the microbiota inhabiting the stone, Int. Biodeterior. 62 (2008) 352–363, https://doi.org/10.1016/j.ibiod.2008.03.002.

[52] F. Jroundi, E.J. Bedmar, C. Rodríguez-Navarro, M.T. González-Muñoz, Consolidation of Ornamental stone by Microbial Carbonatogenesis, in: Proceedings of the Global Stone Congress 2010, Alicante, 2010, pp. 1–5.

[53] M.T. González-Muñoz, Bacterial biomineralization applied to the protection-consolidation of ornamental stone: current development and perspectives, Coalition 15 (2008) 12–18.

[54] M.T. González-Muñoz, N. Ben Omar, M. Martínez-Cañamero, M. Rodríguez-Gallego, A. López-Galindo, J.M. Arias, Struvite and calcite crystallization induced by cellular membranes of *Myxococcus xanthus*, J. Cryst. Growth 163 (1996) 434–439, https://doi.org/10.1016/0022-0248(95)01011-4.

[55] K.B. Chekroun, C. Rodríguez-Navarro, M.T. González-Muñoz, J.M. Arias, G. Cultrone, M. Rodríguez-Gallego, Precipitation and growth morphology of calcium carbonate induced by *Myxococcus xanthus*: implications for recognition of bacterial carbonates, J. Sediment. Res. 74 (6) (2004) 868–876, https://doi.org/10.1306/050504740868.

[56] M.T. González-Muñoz, C. Rodríguez-Navarro, J.M. Martínez-Ruiz, J.M. Arias, M. Merroun, M. Rodríguez-Gallego, Bacterial biomineralization: new insights from *Myxococcus*-induced mineral precipitation, Geol. Soc. Lond. Spec. Publ. 336 (2010) 31–50, https://doi.org/10.1144/SP336.3.

[57] G. Piñar, C. Jiménez-López, K. Sterflinger, J. Ettenauer, F. Jroundi, A. Fernández-Vivas, M.T. González-Muñoz, Bacterial community dynamics during the application of a *Myxococcus xanthus*-inoculated culture medium used for consolidation of ornamental limestone, Microb. Ecol. 60 (2010) 15–28, https://doi.org/10.1007/s00248-010-9661-2.

[58] P. Bosch, G. Ranalli, The safety of biocleaning technologies for cultural heritage, Front. Microbiol. 5 (2014) 155, https://doi.org/10.3389/fmicb.2014.00155.

[59] T.J. Beveridge, R.G.E. Murray, Sites of metal deposition in the cell walls of *Bacillus subtilis*, J. Bacteriol. 141 (1980) 876–887, https://doi.org/10.1128/jb.141.2.876-887.1980.

[60] J.B. Thompson, F.G. Ferris, Cyanobacterial precipitation of gypsum, calcite, and magnesite from natural alkaline lake water, Geology 18 (1990) 995–998, https://doi.org/10.1130/0091-7613(1990)018<0995:CPOGCA>2.3.CO;2.

[61] S. Schultze-Lam, D. Fortin, B.S. Davis, T.J. Beveridge, Mineralization of bacterial surfaces, Chem. Geol. 132 (1996) 171–181, https://doi.org/10.1016/S0009-2541(96)00053-8.

[62] F. Hammes, Urealytic Microbial Calcium Carbonate Precipitation, University of Gent, 2003. PhD Thesis.

[63] K. Simkiss, K.M. Wilbur, Biomineralization. Cell Biology and Mineral Deposition, Academic Press, London, United Kingdom, 1991. ISBN 0126438307.

[64] S. Stocks-Fischer, J.K. Galinat, S.S. Bang, Microbiological precipitation of CaCO3, Soil Biol. Biochem. 31 (1999) 1563–1571, https://doi.org/10.1016/S0038-0717(99)00082-6.

[65] W. Stumm, J.J. Morgan, Aquatic Chemistry: an Introduction Emphasizing Chemical Equilibria in Natural Waters, John Wiley & Sons Ltd., New York, 1981. ISBN 9780471834960.
[66] C. Défarge, J. Trichet, A.M. Jaunet, M. Robert, J. Tribble, F.J. Sansone, Texture of microbial sediments revealed by cryo-scanning electron microscopy, J. Sediment. Res. 66 (1996) 935–947, https://doi.org/10.1306/D4268446-2B26-11D7-8648000102C1865D.
[67] F.G. Ferris, W.S. Fyfe, T.J. Beveridge, Metallic ion binding by *Bacillus subtilis*: implications for the fossilization of microorganisms, Geology 16 (1988) 149–152, https://doi.org/10.1130/0091-7613(1988)016<0149:MIBBBS>2.3.CO;2.
[68] D.A. Brown, D.C. Kamineni, J.A. Sawicki, T.J. Beveridge, Minerals associated with biofilms occurring on exposed rock in a granitic underground research laboratory, Appl. Environ. Microbiol. 60 (1994) 3182–3191, https://doi.org/10.1128/aem.60.9.3182-3191.1994.
[69] K.O. Konhauser, S. Schultze-Lam, F.G. Ferris, W.S. Fyfe, F.J. Longstaffe, T.J. Beveridge, Mineral precipitation by epilithic biofilms in the speed river, ontario, Canada, Appl. Environ. Microbiol. 60 (1994) 549–553, https://doi.org/10.1128/aem.60.2.549-553.1994.
[70] T.J. Beveridge, S.A. Makin, J.L. Kadurugamuwa, Z. Li, Interactions between biofilms and the environment, FEMS Microbiol. Rev. 20 (1997) 291–303, https://doi.org/10.1016/S0168-6445(97)00012-0.
[71] S. Weiner, L. Addali, H.D. Wagner, Materials design in biology, Mater. Sci. Eng. C 11 (2000) 1–8, https://doi.org/10.1016/s0928-4931(00)00141-7.
[72] M. Grimaldi, Search for New surface Active Compounds of Microbial Origin in View of the Development of Biorestoration Techniques, Universitá degli Studi di Firenze, Florence, 2012. PhD Thesis.
[73] Ch Rotgers, J. Llopart, Passat i present de la paleontologia als Hostalets de Pierola, Curatorial 1 (2014) 22–27.
[74] G. Ranalli, J.E. Recchiuti, L. Grazia, Bioluminescence and impedance monitoring to detect the activity of starter cultures during frozen storage, Ann. Microbiol. Enzimol. 48 (1998) 169–180, https://doi.org/10.1007/s10764-016-9895-z.
[75] G. Ranalli, G. Alfano, C. Belli, G. Lustrato, I. Bonadduce, M.P. Colombini, E. Zanardini, P. Abbruscato, F. Cappitelli, C. Sorlini, Biotechnology applied to cultural heritage: biorestoration of frescoes using viable bacterial cells and enzymes, J. Appl. Microbiol. 96 (2005) 73–83, https://doi.org/10.1111/j.1365-2672.2004.02429.x.
[76] S. Marín-Ortega, M.À. Calvo, M.Á. Iglesias-Campos, Correlation tests between relative light unit and colony forming unit for improving adenosine triphosphate bioluminescence analysis in bacterial consolidation treatments on palaeontological heritage, Luminescence 37 (2022) 2129–2138, https://doi.org/10.1002/bio.4403.
[77] B. Perito, L. Biagiotti, S. Daly, A. Galizzi, P. Tiano, G. Mastromei, in: O. Ciferri, P. Tiano, G. Mastromei (Eds.), Bacterial Genes Involved in Calcite Crystal Precipitation, Of Microbes and Art: the Role of Microbial Communities in the Degradation and Protection of Cultural Heritage, Plenum, New York, 2000, pp. 219–230, https://doi.org/10.1007/978-1-4615-4239-1_14.
[78] G. Shama, D.J. Malik, The uses and abuses of rapid bioluminescence-based ATP assays, Int. J. Hyg Environ. Health 216 (2013) 115–125, https://doi.org/10.1016/j.ijheh.2012.03.009.
[79] S. Cameotra, T.C. Dakal, Carbonatogenesis: microbial contribution to the conservation of monuments and artwork of stone, Conserv. Sci. 12 (2012) 79–108, https://doi.org/10.6092/issn.1973-9494/3383.
[80] R.S. Berns, D.H. Alman, L. Reniff, G.D. Snyder, M.R. Balonon-Rosen, Visual determination of supra-threshold color-difference tolerances using probit analysis, Color Res. Appl. 16 (1991) 297–316, https://doi.org/10.1002/col.5080160505.
[81] M. Melgosa, M.M. Pérez, A. Yebra, R. Huertas, E. Hita, Algunas reflexiones y recientes recomendaciones internacionales sobre evaluación de diferencias de color, Opt. Pura Apl. 34 (1) (2001) 1–10. ISSN-e 2171-8814.
[82] J.M. Pereira, Gestión del color en proyectos de digitalización. Barcelona, Marcombo, 2013. ISBN 9788426719652.
[83] L. Gonzalo, M. Díaz, S.J. Gutiérrez, S.J. Perdomo, O.L. Gómez, Obtención de hidroxiapatita sintética por tres métodos diferentes y su caracterización para ser utilizada como sustitutivo óseo, Rev. colomb. cienc. quim. farm. 41 (1) (2012) 50–66. ISSN 0034-7418.
[84] J.W. Morse, in: R.J. Reeder (Ed.), The Kinetics of Calcium Carbonate Dissolution and Precipitation, Carbonates: Mineralogy and Chemistry. Reviews in Mineralogy, vol. 11, Mineralogic Society of America, Washington, D.C., 1983, pp. 227–264, https://doi.org/10.1515/9781501508134-011.
[85] R. Wolbers, Cleaning Painted Surfaces, Aqueous Methods, Archetype Publications, London, 2000. ISBN 9781873132364.
[86] P. Cremonesi, El ambiente acuoso para el tratamiento de obras polícromas. Il Prato, Collana i Talenti. Padova, 2015. ISBN 9788863362695.